

PRECONDITIONING LOW RANK GENERALIZED MINIMAL RESIDUAL METHOD (GMRES) FOR IMPLICIT DISCRETIZATIONS OF MATRIX DIFFERENTIAL EQUATIONS*

SHIXU MENG[†], DANIEL APPELÖ[‡], AND YINGDA CHENG[§]

Abstract. This work proposes a new class of preconditioners for the low rank Generalized Minimal Residual Method (GMRES) for multiterm matrix equations arising from implicit timestepping of linear matrix differential equations. We are interested in computing low rank solutions to matrix equations, e.g. arising from spatial discretization of stiff partial differential equations (PDEs). The low rank GMRES method is a particular class of Krylov subspace method where the iteration is performed on the low rank factors of the solution. Such methods can exploit the low rank property of the solution to save on computational and storage cost.

Of critical importance for the efficiency and applicability of the low rank GMRES method is the availability of an effective low rank preconditioner that operates directly on the low rank factors of the solution and that can limit the iteration count and the maximal Krylov rank.

The preconditioner we propose here is based on the basis update and Galerkin (BUG) method, resulting from the dynamic low rank approximation. It is a nonlinear preconditioner for the low rank GMRES scheme that naturally operates on the low rank factors. Extensive numerical tests show that this new preconditioner is highly efficient in limiting iteration count and maximal Krylov rank. We show that the preconditioner performs well for general diffusion equations including highly challenging problems, e.g. high contrast, anisotropic equations. Further, it compares favorably with the state of the art exponential sum preconditioner. We also propose a hybrid BUG - exponential sum preconditioner based on alternating between the two preconditioners.

1. Introduction. We are interested in computing low rank solutions from implicit discretizations of linear matrix differential equations. The model equation takes the form

$$(1.1) \quad \frac{d}{dt}X(t) = F(X(t), t), \quad X(t) \in \mathbb{R}^{m_1 \times m_2}, \quad X(0) = X_0,$$

where

$$F(X(t), t) = \sum_{j=1}^s A_j X(t) B_j^T + G(t),$$

and $A_j \in \mathbb{R}^{m_1 \times m_1}$, $B_j \in \mathbb{R}^{m_2 \times m_2}$ are sparse or structured matrices where a fast matrix-vector product is known. Further, $G(t) \in \mathbb{R}^{m_1 \times m_1}$ is a given function that is assumed to have a known low rank decomposition. The integer s is assumed not to be too large. Equation (1.1) arises in many applications governed by partial differential equations (PDE) after spatial discretizations have been deployed. Although the present paper only concerns matrix equations, we note that the methodology here was designed with low rank tensor approximation as a future research direction.

Using the method-of-lines approach and by implicit temporal discretizations, we arrive at a multiterm linear matrix equation of the following form

$$(1.2) \quad C_1 X D_1^T + C_2 X D_2^T + \cdots + C_k X D_k^T := \mathcal{A}X = b,$$

where $\mathcal{A} : \mathbb{R}^{m_1 \times m_2} \mapsto \mathbb{R}^{m_1 \times m_2}$ is the associated linear operator. If (1.2) has special structure (for example when it has Lyapunov or Sylvester form), then specialized solvers have been developed [24]. However, in the most generic form (1.2), the standard algorithm consists of transforming the matrix above into vector form

$$(1.3) \quad (D_1 \otimes C_1 + \cdots + D_k \otimes C_k) \text{vec}(X) := \mathcal{A}_v \text{vec}(X) = \text{vec}(b)$$

and then using numerical linear algebra tools to solve (1.3). Here, \otimes denotes the standard matrix Kronecker product and $\text{vec}(X) \in \mathbb{R}^{m_1 m_2}$ denotes the vectorized form of the matrix X . The drawback of this approach

*Submitted to the editors October 11, 2024.

[†]Department of Mathematics, Virginia Tech, Blacksburg, VA 24061 U.S.A. (sgl22@vt.edu).

[‡]Department of Mathematics, Virginia Tech, Blacksburg, VA 24061 U.S.A. (appelo@vt.edu) Research supported by DOE Office of Advanced Scientific Computing Research under the Advanced Research in Quantum Computing program, Award Number DE-SC0025424, NSF DMS-2208164, and Virginia Tech.

[§]Department of Mathematics, Virginia Tech, Blacksburg, VA 24061 U.S.A. (yingda@vt.edu) yingda@vt.edu Research supported by DOE grant DE-SC0023164 and Virginia Tech.

is that special structure of the matrix X , which can potentially save computational storage and cost, will be lost.

In many applications, the solution to (1.1) is of low rank or can be well approximated by a low rank matrix, and we are interested in numerical methods that can exploit this. A prominent class of such methods is low rank Krylov methods, which use low rank truncation within a standard Krylov method for (1.2) or (1.3). Such ideas can also be generalized to tensor linear equations when truncation in specific tensor format is used. For matrix equations, we mention the work of low rank truncation by a greedy approach combined with the Galerkin method [15] and low rank conjugate gradient [25] and the references within. For tensor equations, there are various versions of low rank Krylov solvers, presented in [16, 17, 26], and tensor train Generalized Minimal Residual Method (GMRES) appear in [9, 8]. In particular, [22] presented the tensor train-GMRES or hierarchical Tucker-GMRES for the implicit discretization of nonlinear tensor differential equations. There are several challenges associated with low rank Krylov methods. Low rank truncation results in loss of orthogonality in the Krylov subspace [21, 25] which makes analysis of convergence difficult. Also the key in achieving computational efficiency is to find a preconditioner to achieve fast convergence to avoid excessive growths of the numerical ranks during intermediate iterations [17]. Without a good preconditioner, the intermediate rank can easily explode which defeats the purpose of using low rank approximations. Note that preconditioners for low rank methods are only allowed to operate on the low rank factors of the solution [10, 3]. A prominent technique is to write the approximate inverse as sum of Kronecker products, for example as in the popular exponential sum (ES) preconditioner [12, 13]. Another popular method is the multigrid method, which was used in e.g. [4, 26]. Some other ideas include low-rank tensor diagonal preconditioners for wavelet discretizations [2] and references mentioned within [10, 3].

An important class of methods for computing low rank solutions to time-dependent problems is based on the dynamic low rank approximation (DLRA) [14]. There, by projecting the equation onto the tangent space of the low rank manifold, we can constrain the solution to the fixed rank manifold. In the work of Ceruti et al. [7], the authors proposed the basis update and Galerkin (BUG) method to implement DLRA. This method is shown to have many good properties compared to earlier versions of DLRA schemes, and have been applied and generalized to many applications. However, it is limited to first order in time and the DLRA framework in general incurs the modeling error (the error due to the tangent projection) which cannot be estimated or bounded [1, 18].

This work is motivated by the success of the BUG method as a DLRA for time-dependent problems. We propose to use BUG as a novel preconditioner for low rank GMRES method. This preconditioner in itself can be easily defined according to the BUG procedure, resulting in a non-standard nonlinear preconditioner. We discuss how to effectively incorporate this preconditioner in various types of implicit high order time steppers and how to choose the optimal parameter in its implementations. We verify the performance of the preconditioner by comparing it to the ES preconditioner, and propose a hybrid version of them. Numerical examples including the challenging high contrast, anisotropic equations are considered.

The rest of the paper is organized as follows: in Section 2, we review the low rank GMRES method in its various form. Section 3 reviews the BUG method. In Section 4, we present the new BUG preconditioner and its variants. Section 5 contains simulation results. We conclude the paper in Section 6.

2. Review: low rank GMRES. In this section, we will review the low rank GMRES method for solving matrix equation (1.2). The idea is simple, to equip the well-established method GMRES method [23] by the low rank truncation. Note that there are several variants of low rank GMRES method [4, 9, 8]. Our presentation closely follows the recent work in [8] for tensor train-GMRES.

2.1. GMRES. We begin with the review of the Modified Gram-Schmidt GMRES (MGS-GMRES) for solving linear systems $Ax = b$ with $A \in \mathbb{R}^{n \times n}$, $x \in \mathbb{R}^n$, and $b \in \mathbb{R}^n$. Starting from the initial guess x_0 , MGS-GMRES constructs a series of approximations $x_k = x_0 + r_k$ in Krylov subspace

$$r_k = \operatorname{argmin}_{r \in \mathcal{K}_k(A, r_0)} \|r_0 - Ar\|,$$

with $r_0 = b - Ax_0$ and

$$\mathcal{K}_k(A, r_0) = \operatorname{span} \{r_0, Ar_0, \dots, A^{k-1}r_0\}.$$

To find the minimal residual, a matrix $V_k = [v_1, \dots, v_k] \in \mathbb{R}^{n \times k}$ with orthogonal columns and an upper Hessenberg matrix $\overline{H}_k \in \mathbb{R}^{(k+1) \times k}$ are iteratively constructed using the Arnoldi procedure such that

$\text{span}V_k = \mathcal{K}_k(A, r_0)$ and

$$AV_k = V_{k+1}\overline{H}_k, \quad \text{with} \quad V_{k+1}^T V_{k+1} = I_{k+1}.$$

To proceed, one finds $x_k = x_0 + r_k$ where $r_k = V_k y_k$ and

$$y_k = \underset{y \in \mathbb{R}^k}{\text{argmin}} \|\beta e_1 - \overline{H}_k y\|,$$

where $\beta = \|r_0\|$ and $e_1 = (1, 0, \dots, 0)^T \in \mathbb{R}^{k+1}$ so that

$$\|\beta e_1 - \overline{H}_k y_k\| = \|Ar_k - r_0\| = \|b - Ax_k\|.$$

For the stopping criteria, we follow the the norm-wise backward error for both vector and tensor linear systems [8]

$$\eta_{A,b}(x_k) = \frac{\|Ax_k - b\|}{\|A\|_2 \|x_k\| + \|b\|}.$$

Now we summarize the MGS-GMRES algorithm in Algorithm 2.1.

Algorithm 2.1 MGS-GMRES

Input: A, b, x_0 , GMRES tolerance δ , maximal number of iterations m

Output: Approximate solution x_m

- 1: $r_0 = b - Ax_0, \beta = \|r_0\|, v_1 = r_0/\beta.$
 - 2: **for** $k = 1, 2, \dots, m$ **do**
 - 3: $w = Av_k$
 - 4: **for** $i = 1, 2, \dots, k$ **do**
 - 5: $\overline{H}_{i,k} = \langle v_i, w \rangle$
 - 6: $w = w - \overline{H}_{i,k} v_i$
 - 7: **end for**
 - 8: $\overline{H}_{k+1,k} = \|w\|$
 - 9: $v_{k+1} = w/\overline{H}_{k+1,k}$
 - 10: $y_k = \underset{y \in \mathbb{R}^k}{\text{argmin}} \|\beta e_1 - \overline{H}_k y\|$
 - 11: $x_k = x_0 + V_k y_k$
 - 12: **if** $\eta_{A,b}(x_k) \leq \delta$ **then**
 - 13: Break
 - 14: **end if**
 - 15: **end for**
-

2.2. Low rank GMRES. The idea of the low rank GMRES (lrGMRES) for matrix linear systems to equip MGS-GMRES with the low rank truncation. In the following, we review the lrGMRES for (1.2).

The main idea is to keep every low rank matrix in its singular value decomposition (SVD) form in all computations during lrGMRES,

$$X = USV^T,$$

where $[U, S, V]$ is the SVD of $X \in \mathbb{R}^{m_1 \times m_2}$ where $U \in \mathbb{R}^{m_1 \times r}, S \in \mathbb{R}^{r \times r}$, and $V \in \mathbb{R}^{m_2 \times r}$. In particular, we present in Algorithm 2.2 the computation of $X = U_x S_x V_x^T$ to

$$\mathcal{A}(U_x S_x V_x^T) = U_b S_b V_b^T,$$

with a given linear operator $\mathcal{A} : \mathbb{R}^{m_1 \times m_2} \mapsto \mathbb{R}^{m_1 \times m_2}$, and right hand side $b \in \mathbb{R}^{m_1 \times m_2}$ in SVD form $b = U_b S_b V_b^T$. Compared to Algorithm 2.1, the main feature is the use of a low rank truncation $\mathcal{T}_\epsilon^{sum}$ (which is defined in Algorithm 2.3) to prevent rank explosion during iterations. This operation is also called ‘‘rounding’’ in the tensor literature. In Algorithm 2.3, $\mathcal{T}_\epsilon^{svd}$ simply performs a truncated SVD: for any matrix $A = USV^T$ with $S = \text{diag}(\sigma_1, \dots, \sigma_s)$, then $\mathcal{T}_\epsilon^{svd}(A) = U[:, 1:r] \text{diag}(\sigma_1, \dots, \sigma_r) U[:, 1:r]^T$ such that $(\sum_{j=r+1}^s \sigma_j^2)^{1/2} \leq \epsilon$. The rounding tolerance ϵ has to be chosen smaller than or equal to the lrGMRES tolerance δ according to [8]. It was shown in [8] that this lrGMRES is backward stable for tensor linear systems.

In practice, restart is needed to control the memory of the solver, i.e. maximal Krylov rank. The restarted lrGMRES is presented in Algorithm 2.4.

Algorithm 2.2 lrGMRES

Input: linear map \mathcal{A} , b in SVD form $b = U_b S_b V_b^T$, initial guess in SVD form $x_0 = U_{x0} S_{x0} V_{x0}^T$, rounding tolerance ϵ , GMRES tolerance δ , maximal number of iterations m

Output: $[U_x, S_x, V_x, \text{hasConverged}] = \text{lrGMRES}(\mathcal{A}, U_{x0}, S_{x0}, V_{x0}, U_b, S_b, V_b, \epsilon, \delta, m)$

- 1: $[U_{r0}, S_{r0}, V_{r0}] = \mathcal{T}_\epsilon^{\text{sum}}(b - \mathcal{A}(U_{x0} S_{x0} V_{x0}^T))$, $\beta = \|S_{r0}\|$, $U_1 = U_{r0}$, $S_1 = S_{r0}/\beta$, $V_1 = V_{r0}$.
- 2: **for** $k = 1, \dots, m$ **do**
- 3: $[U_w, S_w, V_w] = \mathcal{T}_\epsilon^{\text{sum}}(\mathcal{A}(U_k S_k V_k^T))$
- 4: **for** $i = 1, \dots, k$ **do**
- 5: $\bar{H}_{i,k} = \langle U_i S_i V_i^T, U_w S_w V_w^T \rangle$
- 6: $[U_w, S_w, V_w] = \mathcal{T}_\epsilon^{\text{sum}}(U_w S_w V_w^T - \bar{H}_{i,k} U_i S_i V_i^T)$
- 7: **end for**
- 8: $[U_w, S_w, V_w] = \mathcal{T}_\epsilon^{\text{sum}}(U_w S_w V_w^T)$
- 9: $\bar{H}_{k+1,k} = \|U_w S_w V_w^T\|$
- 10: $U_{k+1} = U_w$, $S_{k+1} = S_w / \bar{H}_{k+1,k}$, $V_{k+1} = V_w$
- 11: $y_k = \text{argmin}_{y \in \mathbb{R}^k} \|\beta e_1 - \bar{H}_k y\|$
- 12: $[U_x, S_x, V_x] = \mathcal{T}_\epsilon^{\text{sum}}(U_{x0} S_{x0} V_{x0}^T + \sum_{j=1}^k y_k(j) U_j S_j V_j^T)$
- 13: **if** $\eta_{\mathcal{A},b}(U_x S_x V_x^T) \leq \delta$ **then**
- 14: hasConverged = True
- 15: Break
- 16: **end if**
- 17: **end for**

Algorithm 2.3 Truncation sum of low rank matrices $(U_j, S_j, V_j)_{j=1}^m \mapsto U, S, V$

Input: low rank matrices in the form $U_j S_j V_j^T$, $j = 1, \dots, m$ with each S_j being a low rank diagonal matrix, rounding tolerance ϵ

Output: $USV^T = \mathcal{T}_\epsilon^{\text{sum}}(\sum_{j=1}^m U_j S_j V_j^T)$

- 1: Form $U = [U_1, \dots, U_m]$, $S = \text{diag}(S_1, \dots, S_m)$, $V = [V_1, \dots, V_m]$
- 2: Perform column pivoted QR: $[Q_1, R_1, \Pi_1] = \text{qr}(U)$, $[Q_2, R_2, \Pi_2] = \text{qr}(V)$
- 3: Compute the truncated SVD: $\mathcal{T}_\epsilon^{\text{svd}}(R_1 \Pi_1 S \Pi_2^T R_2^T) = USV$
- 4: Form $U \leftarrow Q_1 U$, $V \leftarrow Q_2 V$

2.3. Preconditioner. To speed up the convergence of lrGMRES and limit the intermediate rank growth, we consider the preconditioned lrGMRES with a right preconditioner \mathcal{M} . Namely, we solve $\mathcal{A}\mathcal{M}t = b$ and let $X = \mathcal{M}t$. The preconditioned algorithms are detailed in Algorithm 2.5 and Algorithm 2.6.

The design of the preconditioner for low rank scheme is nontrivial. Besides the standard design principle for preconditioners, we require it to be applied in a dimension by dimension fashion, i.e. it should only operator on low rank factors, with memory and computational time proportionate to the rank of the intermediate iterates. There are a few such candidates in the literature, among which the most well-knowns are ES preconditioner and multigrid preconditioner. Due to the strong dependence on rank [11] the multigrid preconditioner for low rank methods is not as effective as its counterpart for full rank methods. In this paper, we choose to benchmark our method with the ES preconditioner. The details of the ES preconditioner is provided in the Appendix.

3. Review: basis update and Galerkin (BUG) method. In this section, we review an alternative approach for time discretizations of (1.1) in low rank format introduced in [7], the BUG method. This scheme is based on DLRA [14] or Dirac–Frenkel time-dependent variational principle. It was designed to capture a fixed rank solution by projecting the equation onto the tangent space of the fixed rank low rank manifold. In particular, the DLRA solves

$$(3.1) \quad \frac{d}{dt} X(t) = \Pi_{X(t)} F(X(t), t),$$

Algorithm 2.4 Restarted lrGMRES

Input: linear map \mathcal{A} , b in SVD form $b = U_b S_b V_b^T$, initial guess in SVD form $x_0 = U_{x_0} S_{x_0} V_{x_0}^T$, rounding tolerance ϵ , GMRES tolerance δ , maximal number of iterations m , restart parameter maxit

Output: $[U_x, S_x, V_x, \text{hasConverged}] = \text{rlrGMRES}(\mathcal{A}, U_{x_0}, S_{x_0}, V_{x_0}, U_b, S_b, V_b, \epsilon, \delta, m, \text{maxit})$

- 1: $\text{hasConverged} = \text{False}$, $i = 1$, $[U_x, S_x, V_x] = [U_{x_0}, S_{x_0}, V_{x_0}]$
- 2: **while** $\text{hasConverged} = \text{False}$ & $i \leq \text{maxit}$ **do**
- 3: $[U_x, S_x, V_x, \text{hasConverged}] = \text{lrGMRES}(\mathcal{A}, U_x, S_x, V_x, U_b, S_b, V_b, \epsilon, \delta, m)$
- 4: $i = i + 1$
- 5: **end while**

Algorithm 2.5 Preconditioned lrGMRES

Input: linear map \mathcal{A} , b in SVD form $b = U_b S_b V_b^T$, initial guess in SVD form $x_0 = U_{x_0} S_{x_0} V_{x_0}^T$, rounding tolerance ϵ , GMRES tolerance δ , maximal number of iterations m , preconditioner \mathcal{M}

Output: $[U_x, S_x, V_x, \text{hasConverged}] = \text{plrGMRES}(\mathcal{A}, \mathcal{M}, U_{x_0}, S_{x_0}, V_{x_0}, U_b, S_b, V_b, \epsilon, \delta, m)$

- 1: $[U_{r_0}, S_{r_0}, V_{r_0}] = \mathcal{T}_\epsilon^{\text{sum}}(b - \mathcal{A}(U_{x_0} S_{x_0} V_{x_0}^T))$, $\beta = \|S_{r_0}\|$, $U_1 = U_{r_0}$, $S_1 = S_{r_0}/\beta$, $V_1 = V_{r_0}$.
- 2: **for** $k = 1, \dots, m$ **do**
- 3: $[U_w, S_w, V_w] = \mathcal{T}_\epsilon^{\text{sum}}(\mathcal{A}\mathcal{M}(U_k S_k V_k^T))$
- 4: **for** $i = 1, \dots, k$ **do**
- 5: $\bar{H}_{i,k} = \langle U_i S_i V_i^T, U_w S_w V_w^T \rangle$
- 6: $[U_w, S_w, V_w] = \mathcal{T}_\epsilon^{\text{sum}}(U_w S_w V_w^T - \bar{H}_{i,k} U_i S_i V_i^T)$
- 7: **end for**
- 8: $[U_w, S_w, V_w] = \mathcal{T}_\epsilon^{\text{sum}}(U_w S_w V_w^T)$
- 9: $\bar{H}_{k+1,k} = \|U_w S_w V_w^T\|$
- 10: $U_{k+1} = U_w$, $S_{k+1} = S_w / \bar{H}_{k+1,k}$, $V_{k+1} = V_w$
- 11: $y_k = \text{argmin}_{y \in \mathbb{R}^k} \|\beta e_1 - \bar{H}_k y\|$
- 12: $[U_e, S_e, V_e] = \mathcal{T}_\epsilon^{\text{sum}}\left(\sum_{j=1}^k y_k(j) U_j S_j V_j^T\right)$
- 13: $[U_{Me}, S_{Me}, V_{Me}] = \mathcal{T}_\epsilon^{\text{sum}}(\mathcal{M}(U_e S_e V_e^T))$
- 14: $[U_x, S_x, V_x] = \mathcal{T}_\epsilon^{\text{sum}}(U_{x_0} S_{x_0} V_{x_0}^T + U_{Me} S_{Me} V_{Me}^T)$
- 15: **if** $\eta_{\mathcal{A},b}(U_x S_x V_x^T) \leq \delta$ **then**
- 16: $\text{hasConverged} = \text{True}$
- 17: **Break**
- 18: **end if**
- 19: **end for**

where $\Pi_{X(t)}$ is the orthogonal projection onto the tangent space $T_{X(t)}\mathcal{M}_r$ of the the rank r matrix manifold $\mathcal{M}_r = \{X \in \mathbb{R}^{m_1 \times m_2}, \text{rank}(X) = r\}$ at $X(t)$. For completeness, we include a description of the BUG method for solving (1.1) in Algorithm 3.1. In Algorithm 3.1, first, two subproblems that come from the projector splitting of DLRA [19] are solved in the K- and L-step, identifying the row and column spaces. Then, a Galerkin evolution step is performed in the resulting space, searching for the optimal solution with the Galerkin condition. This method is first order in time and fixed in rank. Later improvements to the method includes the rank adaptive version [6], and second or higher order variations [20, 5]. The BUG method performs well in many applications. However, it suffers from the modeling error from the tangent projection [1] and this error can not be bounded or estimated [1, 18].

4. Proposed methods: BUG preconditioner and variants. Motivated by the success of BUG method for many applications, we propose to use it as a preconditioner for low rank GMRES scheme. The low rank feature of BUG method makes it suitable as a preconditioner for low rank schemes. With the GMRES framework, it no long suffers the shortcomings of convergence due to the modeling error. Below, we will describe the BUG preconditioner for various implicit time discretizations. Then we will propose a hybrid preconditioner combining BUG and the standard ES preconditioners.

Algorithm 2.6 Restarted preconditioned lrGMRES

Input: linear map \mathcal{A} , b in SVD form $b = U_b S_b V_b^T$, initial guess in SVD form $x_0 = U_{x_0} S_{x_0} V_{x_0}^T$, rounding tolerance ϵ , GMRES tolerance δ , maximal number of iterations m , restart parameter maxit , preconditioner \mathcal{M}

Output: $[U_x, S_x, V_x, \text{hasConverged}] = \text{rplrGMRES}(\mathcal{A}, \mathcal{M}, U_{x_0}, S_{x_0}, V_{x_0}, U_b, S_b, V_b, \epsilon, \delta, m, \text{maxit})$

1: $\text{hasConverged} = \text{False}$, $i = 1$, $[U_x, S_x, V_x] = [U_{x_0}, S_{x_0}, V_{x_0}]$

2: **while** $\text{hasConverged} = \text{False}$ & $i \leq \text{maxit}$ **do**

3: $[U_x, S_x, V_x, \text{hasConverged}] = \text{plrGMRES}(\mathcal{A}, \mathcal{M}, U_x, S_x, V_x, U_b, S_b, V_b, \epsilon, \delta, m)$

4: $i = i + 1$

5: **end while**

Algorithm 3.1 BUG integrator using implicit Euler for $\frac{d}{dt}X = F(X, t)$ [7].

Input: numerical solution at t^n : rank r matrix \hat{X}^n in its SVD form $U^n \Sigma^n (V^n)^T$.

Output: numerical solution at t^{n+1} : rank r matrix \hat{X}^{n+1} in its SVD form $U^{n+1} \Sigma^{n+1} (V^{n+1})^T$.

1: Prediction. K-step and L-step integrating from t^n to t^{n+1} .

Solve

$$K^{n+1} - K^n = \Delta t F(K^{n+1} (V^n)^T, t) V^n, \quad K^n = U^n \Sigma^n,$$

to obtain K^{n+1} , and $[\tilde{U}, \sim, \sim] = \text{qr}(K^{n+1})$.

Solve

$$L^{n+1} - L^n = \Delta t F(U^n (L^{n+1})^T, t)^T U^n, \quad L^n = V^n \Sigma^n,$$

to obtain L^{n+1} , and $[\tilde{V}, \sim, \sim] = \text{qr}(L^{n+1})$.

2: Galerkin Evolution. S-step: solve for S^{n+1} from

$$S^{n+1} - S^n = \Delta t \tilde{U}^T F(\tilde{U} S^{n+1} \tilde{V}^T, t) \tilde{V}, \quad S^n = \tilde{U}^T U^n \Sigma^n (V^n)^T \tilde{V},$$

to obtain S^{n+1} .

3: Output. $\hat{X}^{n+1} = \tilde{U} S^{n+1} \tilde{V}^T = U^{n+1} \Sigma^{n+1} (V^{n+1})^T$.

4.1. BUG preconditioner and implicit time stepping. Implicit time stepping of the matrix differential equations (1.1) will yield matrix equations in the form $\mathcal{A}X = b$. This can be preconditioned by the BUG methodology as described in Algorithm 4.1. Starting with an input of an initial guess USV^T with rank r , the preconditioner $\mathcal{M}_{\text{BUG}}^{A,U,S,V}$ computes a low rank solution $U_{\text{new}} S_{\text{new}} V_{\text{new}}^T$ with the same rank r . We note that in the K-, L- and Galerkin steps, smaller systems (of size $m_1 \times r, m_2 \times r, r \times r$) need to be solved respectively. With the assumption that r being small, and the projected equations being better conditioned, those will be amenable for fast computations. We would like to emphasize that this is an unconventional preconditioner because the algorithm depends on the choice of U, S, V , and when used, e.g. in Algorithm 4.2 it is a nonlinear mapping unlike most other preconditioners.

In this work, we consider the following time discretizations.

- **Implicit midpoint:** in the implicit midpoint method, we solve

$$(4.1) \quad X^{n+1} - \Delta t \left(\theta \sum_{j=1}^s A_j X^{n+1} B_j^T + 1/2 \sum_{j=1}^s A_j X^n B_j^T + G^n \right) = X^n,$$

where $G^n = G(x, y, (t_n + t_{n+1})/2)$.

- **l -step BDF (backward differentiation formula) time stepping:** the BDF time stepping leads to

$$(4.2) \quad X^{n+1} - \Delta t \beta \left(\sum_{j=1}^s A_j X^{n+1} B_j^T + G^{n+1} \right) = \sum_{j=0}^l \alpha_j X^{n-j},$$

where α_j, β are coefficients for BDF scheme.

Algorithm 4.1 BUG preconditioner for $\mathcal{A}X = b$ **Input:** linear map \mathcal{A} , the right hand side b , initial guess in SVD form USV^T **Output:** $[U_{\text{new}}, S_{\text{new}}, V_{\text{new}}] = \mathcal{M}_{\text{BUG}}^{\mathcal{A}, U, S, V}(b)$ 1: K-step: set $K_0 = bV$, solve

$$\mathcal{A}(K_1 V^T)V = K_0$$

to obtain $[U, \sim, \sim] = \text{qr}(K_1)$.2: L-step: set $L_0 = b^T U$, solve

$$\mathcal{A}^T(L_1 U^T)U = L_0$$

to obtain $[V, \sim, \sim] = \text{qr}(L_1)$. Here $\mathcal{A}^T(L_1 U^T) := (\mathcal{A}(U L_1^T))^T$.3: Galerkin: set $\Sigma_0 = U^T bV$, solve

$$U^T \mathcal{A}(U \Sigma_1 V^T)V = \Sigma_0$$

and obtain $[U_c, S_c, V_c] = \text{svd}(\Sigma_1)$.4: Obtain $U_{\text{new}} = U U_c$, $V_{\text{new}} = V V_c$, $S_{\text{new}} = S_c$.

- **Diagonally implicit Runge–Kutta (DIRK) time stepping:** The l -stage DIRK method means we solve from $i = 1, \dots, l$

$$(4.3) \quad X^{(i)} - \Delta t \left(a_{ii} F(X^{(i)}, t^n + c_i \Delta t) + \sum_{j=1}^{i-1} a_{ij} F(X^{(j)}, t^n + c_j \Delta t) \right) = X^n,$$

and

$$X^{n+1} = X^n + \Delta t \sum_{j=1}^l b_j F(X^{(j)}, t^n + c_j \Delta t),$$

where the coefficients a_{ij}, c_j, b_i are given by the Butcher tableau, and $F(X, t) = \sum_{j=1}^s A_j X B_j^T + G(t)$.**Algorithm 4.2** Implicit Midpoint Method with lrGMRES with BUG preconditioner**Input:** A set of second-order finite difference matrices $\{A_j, B_j\}_{j=1}^s$, time discretization parameters $\Delta t, n_t$ and θ , initial condition in SVD form $X_0 = U_0 S_0 V_0^T$, source $G(t)$, rounding tolerance for lrGMRES ϵ , truncation tolerance ϵ_2 , lrGMRES stopping criteria δ , maximal number of iterations m , restart parameter maxit , preconditioner \mathcal{M} **Output:** Solution at final time $[U, S, V]$ 1: Set the linear map \mathcal{A} by $\mathcal{A}X = X - \Delta t \theta \sum_{j=1}^s A_j X B_j^T$.2: Initialization: $U = U_0, S = S_0, V = V_0$ 3: **for** $n = 1, \dots, n_t$ **do**4: $t = (n - 1)\Delta t$ 5: $X \leftarrow USV^T, G_\theta \leftarrow G(\cdot, \cdot, (1 - \theta)t + \theta(t + \Delta t)), U_b S_b V_b^T \leftarrow \Delta t(1 - \theta) \sum_{j=1}^s A_j X B_j^T + G_\theta^n + X$ 6: $\mathcal{M} \leftarrow \mathcal{M}_{\text{BUG}}^{\mathcal{A}, U, S, V}$ 7: $[U, S, V, \text{hasConverged}] \leftarrow \text{rplrGMRES}(\mathcal{A}, \mathcal{M}, U, S, V, U_b, S_b, V_b, \epsilon, \delta, m, \text{maxit})$ 8: $[U, S, V] \leftarrow \mathcal{T}_{\epsilon_2}^{\text{sum}}(USV^T)$ 9: **end for**

These methods can be readily combined with the low rank GMRES solver with BUG preconditioner, see for example Algorithm 4.2, where the implicit midpoint method is provided as an example. In the following, we would like to discuss several key design features of the BUG preconditioner applied to matrix equations arising from the aforementioned time discretizations.

First, we discuss the choice of U, S, V in the BUG preconditioner, and we note that USV^T is also used as the initial guess of the low rank GMRES iteration. The choice is according to the following.

- For the implicit midpoint schemes, $USV^T = X^n$ is the numerical solution at time step n .
- For the BDF scheme, $USV^T = \sum_{j=0}^l a_j X^{n-j}$ is a linear combination of computed solutions at previous steps.

- For the DIRK scheme, at the j -th inner stage, we take $USV^T = X^{n-1,(j)}$ which is the numerical solution at the j -th inner stage of the previous time steps. This choice is critical for the performance of the DIRK method and will be studied in detail in Example 5.8.

For the stopping criteria, we follow [8] and use

$$\eta_{\mathcal{A},b}(x_k) = \frac{\|\mathcal{A}x_k - b\|}{\|\mathcal{A}\|_2\|x_k\| + \|b\|} \leq \delta,$$

where $\|\mathcal{A}\|_2$ is estimated as follows. Choose a set W of normalized matrices w generated randomly from a normal and uniform distribution, we estimate

$$\|\mathcal{A}\|_2 = \max_{w \in W} \|\mathcal{A}w\|.$$

In our algorithm, we choose 10 normally distributed matrices and 10 uniformly distributed matrices. Such a stopping criteria may ensure a backward stable solution in contrast to using $\eta_b(x_k) = \|\mathcal{A}x_k - b\|/\|b\|$ as was pointed out by [8]. The stopping parameter of lrGMRES is chosen as $\delta = \epsilon$ which was recommended in [8].

Finally, we want to discuss the choice of the rounding tolerance ϵ in low rank GMRES. This is chosen according to the local truncation errors of the scheme. In Section 5, we provide details for such choice for various kinds of discretizations. Here, let's focus on an example of the application of Algorithm 4.2 for solving (1.1) arising from a diffusion type of partial differential equation with second order spatial discretizations. The details of the setup and numerical results are reported in Section 5.1. We assume the time step and spatial mesh is on the same order, i.e. $\Delta t = O(h)$, where h is the spatial mesh in both x and y direction. In this case the local truncation error is on the order of $\Delta t(\Delta t^2 + h^2) = O(h^3)$. A pessimistic estimate of the local truncation error caused by an ϵ truncation in the solution matrix X is $h\epsilon(1 + \Delta t/h^2)$. Here, we note the h factor is needed to convert matrix norm to solution norm. This is because for a 2D function $f(x, y)$, the L^2 norm $\sqrt{\int f(x, y)^2 dx dy} = Ch\|F\|$, where the matrix $F_{ij} = F(x_i, y_j)$. Recall that the rounding tolerance ϵ in the lrGMRES is to make sure that its induced error is on the same order of the local truncation error. From $h\epsilon(1 + \Delta t/h^2) = O(h^3)$, we obtain $\epsilon = O(h^3)$. Similarly, we take $\epsilon_2 = O(h^2)$ for the truncation parameter in Line 8 in Algorithm 4.2 to match the local truncation error (considering the rescaling of matrix norm and solution norm). The 2-norm of the operator \mathcal{A} is expected to be bounded by $C\frac{\Delta t}{h^2}$ for linear diffusion type equations which are weakly perturbations of isotropic diffusion equation with constant coefficients, since for $\text{vec}(\mathcal{A}X) = (I \otimes I - \frac{1}{2}\Delta t(I \otimes D + D \otimes I))\text{vec}(X)$, the 2-norm of the operator \mathcal{A} is bounded by $C\frac{\Delta t}{h^2}$; here D is the second-order finite difference matrix whose condition number scales as $1/h^2$. With those parameter choices, we have the following results on stability and convergence of the numerical method.

THEOREM 4.1 (Stability). *Suppose the matrix differential equation (1.1) satisfies one-sided Lipschitz condition*

$$\langle F(X, t) - F(Y, t), X - Y \rangle \leq \alpha\|X - Y\|^2.$$

The implicit midpoint method with low rank GMRES scheme as described in Algorithm 4.2 applied to a linear diffusion type problem with the property $\|\mathcal{A}\|_2 \leq \frac{C\Delta t}{h^2}$, and mesh size $\Delta t = O(h)$, tolerance $\epsilon = O(h^3)$, $\epsilon_2 = O(h^2)$ is stable if Line 7 converges for all time steps, i.e. we have

$$\|X^n\| \leq C\|X^0\|.$$

Here, the matrix inner product is defined as $\langle A, B \rangle = \sum_{i,j} a_{ij}b_{ij}$ and $\|\cdot\|$ denotes the Frobenious norm. C is a generic constant that does not depend on mesh size $\Delta t, h$.

Proof. Let's define the intermediate solution from Line 7 in Algorithm 4.2 as \tilde{X}^{n+1} . Then $X^{n+1} = \mathcal{T}_{\epsilon_2}^{\text{sum}}(\tilde{X}^{n+1})$, and $\|X^{n+1}\| \leq \|\tilde{X}^{n+1}\|$ due to the property of the truncated SVD. We denote $r^n = \tilde{X}^{n+1} - X^n - \Delta t F\left((X^n + \tilde{X}^{n+1})/2, t^{n+1/2}\right)$, which is the residual from the low rank GMRES. From the stopping criteria and the fact that it has converged, and $\delta = \epsilon$, we have

$$(4.4) \quad \|r^n\| \leq \epsilon(\|\mathcal{A}\|_2\|\tilde{X}^{n+1}\| + \|b\|) \leq C\Delta t^2(\|\tilde{X}^{n+1}\| + \|X^n\|),$$

where we have used the definition of b from (4.1). Now we apply the inner product with $\tilde{X}^{n+1} + X^n$ to the residual equation, and we have

$$\begin{aligned} \|\tilde{X}^{n+1}\|^2 - \|X^n\|^2 &= \langle \tilde{X}^{n+1} - X^n, \tilde{X}^{n+1} + X^n \rangle \\ &= \left\langle \Delta t F \left((X^n + \tilde{X}^{n+1})/2, t^{n+1/2} \right) + r^n, \tilde{X}^{n+1} + X^n \right\rangle \\ &\leq \alpha \Delta t / 2 \|X^n + \tilde{X}^{n+1}\|^2 + \|r^n\| \|X^n + \tilde{X}^{n+1}\| \\ &\leq C \Delta t (\|X^n\|^2 + \|\tilde{X}^{n+1}\|^2) \end{aligned}$$

where we used (4.4) in the last line. Then it is straightforward to see $\|X^{n+1}\| \leq \|\tilde{X}^{n+1}\| \leq (1 + C\Delta t)\|X^n\|$ and the theorem follows. \square

THEOREM 4.2 (Convergence). *Under the same assumptions as in the previous theorem, the implicit midpoint method with low rank GMRES scheme as described in Algorithm 4.2 is convergent of second order, i.e.*

$$(4.5) \quad \|X^n - X(t^n)\| \leq C\Delta t.$$

with an initial condition satisfying $\|X^n - X(t^n)\| \leq Ch$. Here, $X(t^n)$ denotes the exact solution at t^n . C is a generic constant that does not depend on mesh size $\Delta t, h$. We notice that (4.5) implies second order because of the matrix and function norm conversion $\sqrt{\int (f(x, y))^2 dx dy} = Ch\|F\|$.

Proof. We use the same notation as in the proof of the previous theorem. (4.4) now gives $\|r^n\| \leq C\Delta t^2$ using the stability result.

We define the error $e^n = X^n - X(t^n)$, and $\tilde{e}^n = \tilde{X}^n - X(t^n)$. For the exact solution, we have

$$X(t^{n+1}) - X(t^n) = \Delta t F \left((X(t^n) + X(t^{n+1}))/2, t^{n+1/2} \right) + G^n,$$

where $G^n = C\Delta t^2$ from local truncation analysis, $\Delta t = O(h)$ and matrix and solution norm rescaling. By the linearity of $F(\cdot, t)$, we easily get

$$\tilde{e}^{n+1} - e^n = \Delta t F \left((e^n + \tilde{e}^{n+1})/2, t^{n+1/2} \right) + r^n - G^n.$$

Therefore,

$$\begin{aligned} \|\tilde{e}^{n+1}\|^2 - \|e^n\|^2 &= \langle \tilde{e}^{n+1} - e^n, \tilde{e}^{n+1} + e^n \rangle \\ &= \left\langle \Delta t F \left((e^n + \tilde{e}^{n+1})/2, t^{n+1/2} \right) + r^n - G^n, \tilde{e}^{n+1} + e^n \right\rangle \\ &\leq \alpha \Delta t / 2 \|e^n + \tilde{e}^{n+1}\|^2 + C\Delta t^2 \|e^n + \tilde{e}^{n+1}\| \\ &\leq \alpha \Delta t (\|e^n\|^2 + \|\tilde{e}^{n+1}\|^2) + \Delta t (\|e^n\|^2 + \|\tilde{e}^{n+1}\|^2) + C\Delta t^3. \end{aligned}$$

When Δt is small enough, we have $\|\tilde{e}^{n+1}\|^2 \leq (1 + C\Delta t)\|e^n\|^2 + C\Delta t^3$. Now we use $e^{n+1} = \tilde{e}^{n+1} + X^n - \tilde{X}^n$. Since $\|X^n - \tilde{X}^n\| \leq \epsilon_2 = C\Delta t^2$, we get $\|e^{n+1}\|^2 \leq (1 + C\Delta t)\|e^n\|^2 + C\Delta t^3$. This implies (4.5) with the assumption on initial condition. \square

We note that the theorems above works for general preconditioners, i.e. BUG and also ES preconditioners. It serves as a guideline and assurance on our parameter choice, which will be numerically verified in Section 5.

4.2. Hybrid preconditioner. We now propose a hybrid preconditioner of the ES and the BUG preconditioner. The ES preconditioner is a well known preconditioner for low rank iterative solvers. It has a simple and direct construction, which has shown effectiveness in many high dimensional applications for tensor equations [3]. The detail of this preconditioner is reported in the Appendix. The definition of the hybrid preconditioner is straightforward. It alternates between the two preconditioners (e.g. restart=1) which is reported in Algorithm 4.3. We have also considered other restart parameter, but do not observe significant difference. The main motivation for the hybrid preconditioner is to use the ES to provide a better

Algorithm 4.3 Restarted lrGMRES with hybrid preconditioner

Input: linear map \mathcal{A} , b in SVD form $b = U_b S_b V_b^T$, initial guess in SVD form $x_0 = U_{x_0} S_{x_0} V_{x_0}^T$, rounding tolerance ϵ , GMRES tolerance δ , maximal number of iterations m , number of restart maxit , preconditioner \mathcal{M}

Output: $[U_x, S_x, V_x, \text{hasConverged}] = \text{rplrGMRES}(\mathcal{A}, \mathcal{M}_{\text{hybrid}}, U_{x_0}, S_{x_0}, V_{x_0}, U_b, S_b, V_b, \epsilon, \delta, m, \text{maxit})$

```

1: hasConverged = False,  $i = 1$ ,  $[U_x, S_x, V_x] = [U_{x_0}, S_{x_0}, V_{x_0}]$ 
2: while hasConverged = False &  $i \leq \text{maxit}$  do
3:   if  $i == 1 \pmod{2}$  then
4:      $[U_x, S_x, V_x, \text{hasConverged}] = \text{plrGMRES}(\mathcal{A}, \mathcal{M}_{\text{ES}}, U_x, S_x, V_x, U_b, S_b, V_b, \epsilon, \delta, m)$ 
5:   else  $i == 0 \pmod{2}$ 
6:      $[U_x, S_x, V_x, \text{hasConverged}] = \text{plrGMRES}(\mathcal{A}, \mathcal{M}_{\text{BUG}}^{A, U_x, S_x, V_x}, U_x, S_x, V_x, U_b, S_b, V_b, \epsilon, \delta, m)$ 
7:   end if
8:    $i = i + 1$ 
9: end while

```

initial guess for the BUG update and vice versa. We note that this is different from the flexible GMRES framework, because the BUG preconditioner is nonlinear.

Finally, we remark that it is also possible to use the rank adaptive version of BUG method [6] as a preconditioner. The essential design of the schemes are very similar. We have tried this in numerical tests, and did not find significant advantages. Thus the results are not reported in this paper.

5. Numerical results. In this section, we test the proposed numerical methods by considering the diffusion equation with variable coefficients

$$(5.1) \quad \begin{aligned} \frac{\partial X}{\partial t} = & b_1(y) \frac{\partial}{\partial x} \left(a_1(x) \frac{\partial X}{\partial x} \right) + b_2(y) \frac{\partial^2 (a_2(x) X)}{\partial x \partial y} \\ & + a_3(x) \frac{\partial^2 (b_3(y) X)}{\partial x \partial y} + a_4(x) \frac{\partial}{\partial y} \left(b_4(y) \frac{\partial X}{\partial y} \right) + G(x, y, t) \end{aligned}$$

on the square domain $[-1, 1]^2$ subject to zero Dirichlet boundary conditions and a given initial condition. We discretize the equation by standard finite difference in space and implicit time integrators with various order. The spatially discretized scheme of (5.1) is then an example of (1.1). Let the time grids be

$$t_k = k\Delta t, \quad k = 0, 1, \dots, n_t,$$

for some integer $n_t > 0$, and the space grids be

$$(x_i, y_j) = (-1 + i\Delta x, -1 + j\Delta y), \quad i = 1, \dots, n_x, \quad j = 1, \dots, n_y,$$

for some integers $n_x > 0$ and $n_y > 0$. The unknown is represented by a time dependent matrix $X_{i,j}^n \approx X(x_i, y_j, t_n)$.

5.1. Parameter study for the BUG preconditioner . In this subsection, we verify the optimal parameter for the BUG preconditioner by numerical experiments. We consider (5.1) with

$$(5.2) \quad \begin{aligned} a_1(x) &= 1 + 0.1 \sin(\pi x), & b_1(y) &= 1 + 0.1 \cos(\pi y), \\ a_2(x) &= 0.15 + 0.1 \sin(\pi x), & b_2(y) &= 0.15 + 0.1 \cos(\pi y), \\ a_3(x) &= 0.15 + 0.1 \cos(\pi x), & b_3(y) &= 0.15 + 0.1 \sin(\pi y), \\ a_4(x) &= 1 + 0.1 \sin(\pi x), & b_4(y) &= 1 + 0.1 \cos(\pi y), \end{aligned}$$

and the rank 1 manufactured solution given by

$$(5.3) \quad X(x, y, t) = 0.1 \exp(-x^2/0.15^2) \exp(-y^2/0.15^2) \exp(-t),$$

which will implicit define the forcing term $G(x, y, t)$. The final time is $t_{\text{end}} = 0.1\pi$. We carry out the computation on four different grids with $n_x = n_y \in \{2^5 - 1, 2^6 - 1, 2^7 - 1, 2^8 - 1\}$. The timestep is chosen

according to $n_t = \lfloor t_{\text{end}}/h_x \rfloor$ and $\Delta t = t_{\text{end}}/n_t$ with final time $t_{\text{end}} = 0.1\pi$. We test with the second order spatial discretization and implicit midpoint method in time with time step choice $\Delta t = O(h)$.

The parameters we test include the following: restart parameter, rounding tolerance ϵ and stopping criteria. For the restart parameter, to control the rank growth, we implement the restarted-lrGMRES where the lrGMRES restart every three iterations with a maximal total number of iterations as 90. We will illustrate by an example that frequent restarting will actually help bring the iteration numbers for the preconditioner down. This seems to be a feature of this nonlinear preconditioner.

As for the parameter ϵ , according to the discussions in Section 4.1, we use $\epsilon = h^2$ in the lrGMRES and $\epsilon_2 = O(h^2)$. As for the stopping criteria, we follow [8] and use

$$\eta_{\mathcal{A},b}(x_k) = \frac{\|\mathcal{A}x_k - b\|}{\|\mathcal{A}\|_2\|x_k\| + \|b\|} \leq \delta,$$

where $\|\mathcal{A}\|_2$ is estimated as follows. Choose a set W of normalized matrices w generated randomly from a normal and uniform distribution, we estimate

$$\|\mathcal{A}\|_2 = \max_{w \in W} \|\mathcal{A}w\|.$$

In our algorithm, we choose 10 normally distributed matrices and 10 uniformly distributed matrices. Such a stopping criteria may ensure a backward stable solution in contrast to using $\eta_b(x_k) = \|\mathcal{A}x_k - b\|/\|b\|$ as was pointed out by [8]. The stopping parameter of lrGMRES is chosen as $\delta = \epsilon$ which was recommended in [8].

The discussions above are the baseline for the ‘‘optimal’’ parameter choice. Below, we provide the numerical results based on this choice first. Then we will vary each individual parameter and observe the difference in the numerical performance.

EXAMPLE 5.1 (Optimal parameter). We solve (5.1) with variable coefficients (5.2) and manufactured solution (5.3). We now provide the numerical results using the optimal parameters mentioned above, namely restart parameter being three, stopping criteria $\eta_{\mathcal{A},b}(x_k) \leq \delta, \delta = \epsilon = h^3$. The second order convergence can be clearly observed in Table 1. Figure 1 displays, at each time step, the solution error, $\eta_{\mathcal{A},b}$, the solution rank, the maximal Krylov rank, and the iteration number. It is evident that the preconditioner is effective. The number of iteration is mostly 1 except the initial time step. The numerical solution is of low rank, and more importantly, the maximal Krylov rank remains low.

We compare lrGMRES with BUG preconditioner and lrGMRES without any preconditioner in Figure 2, where we display the history of solution error, iteration number, and maximal Krylov rank. It is evident that the preconditioner is the key to feasible computational cost.

h	error	order
3.12(-2)	1.06(-4)	-
1.56(-2)	2.71(-5)	1.97
7.81(-3)	6.78(-6)	2.00
3.90(-3)	1.77(-6)	1.93

Table 1: Example 5.1. Solving diffusion equation with variable coefficients (5.2) and manufactured solution (5.3) with BUG preconditioner. Restart every 3 iterations. Stopping criteria $\eta_{\mathcal{A},b}(x_k) \leq \delta, \delta = \epsilon = h^3$. For $h = h_x = h_y \in \{3.12(-2), 1.56(-2), 7.81(-3), 3.90(-3)\}$, this table displays the solution error at the final time and order of convergence.

EXAMPLE 5.2 (Varying the restart parameter). In this example, we enlarge the restart parameter to 25 while keeping all other parameters unchanged from Example 5.1. We solve (5.1) with variable coefficients (5.2) and manufactured solution (5.3). Figure 3 displays the corresponding result. The iteration numbers increase dramatically for the first time step, and the maximal Krylov ranks also become larger. This shows that BUG preconditioning benefits from frequent restarting.

EXAMPLE 5.3 (Varying the stopping criteria). In this example, we switch the stopping criteria to η_b and keep all other parameters the same as in Example 5.1. The results for (5.1) with variable coefficients

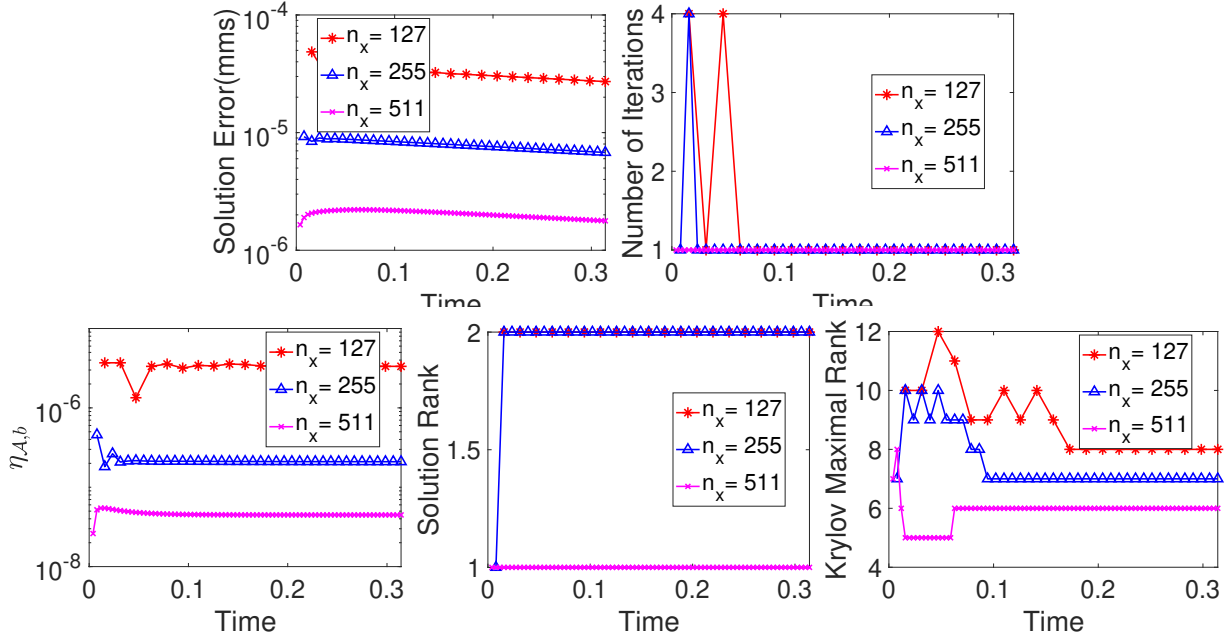


Fig. 1: Example 5.1. Solving diffusion equation with variable coefficients (5.2) and manufactured solution (5.3) with BUG preconditioner. Restart every 3 iterations. Stopping criteria $\eta_{\mathcal{A},b}(x_k) \leq \delta$. $\delta = \epsilon = h^3$. For $h = h_x = h_y \in \{1.56(-2), 7.81(-3), 3.90(-3)\}$, this figure displays the history of solution error, iteration number, $\eta_{\mathcal{A},b}$, solution rank, and maximal Krylov rank.

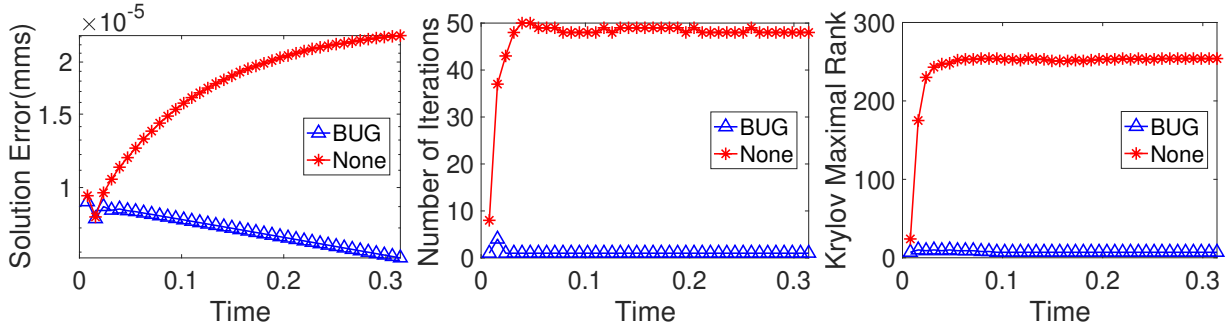


Fig. 2: Example 5.1. Solving diffusion equation with variable coefficients (5.2) and manufactured solution (5.3) with BUG preconditioner (which restarts every 3 iterations) and no preconditioner (which restarts every 3 iterations “None-3” and every 25 iterations “None-25”). Stopping criteria $\eta_{\mathcal{A},b}(x_k) \leq \delta$. $\delta = \epsilon = h^3$. For $h = h_x = h_y \in \{7.81(-3)\}$, this figure displays the history of solution error, iteration number, and maximal Krylov rank.

(5.2) and manufactured solution (5.3) are reported in Figure 4 when the mesh size $h = 7.81(-3)$. In this case, the iteration numbers are drastically larger, i.e., the stopping criteria $\eta_b \leq \delta$ does not guarantee that η_b stagnates below the stopping parameter before the maximal number of iteration is reached. Similar behavior has been reported in [8].

EXAMPLE 5.4 (Varying the rounding tolerance). In this example, we solve (5.1) with variable coefficients (5.2) and manufactured solutions given by (5.3). To test whether second-order convergence may be observed by a larger rounding tolerance, we chose a larger rounding tolerance $\epsilon = h^2$, while keeping all other parameters same as Example 5.1. The convergence rate is displayed in Table 2 for both ES and BUG preconditioner. We observe clearly deteriorated convergence rate (of first order) for ES preconditioners.

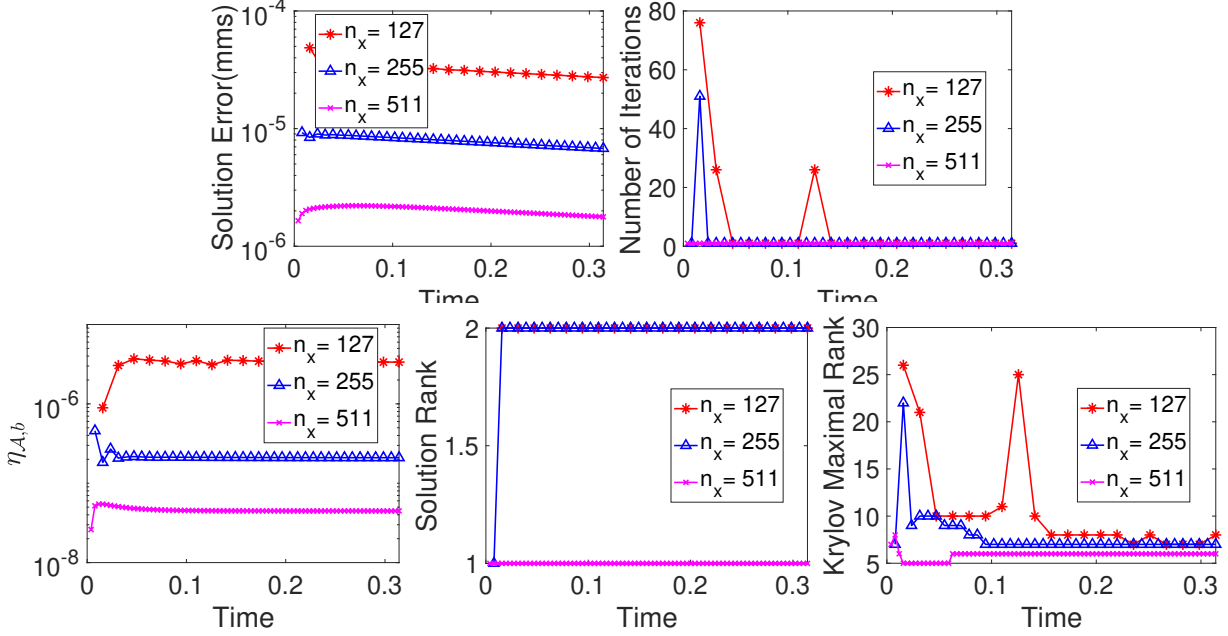


Fig. 3: Example 5.2. Solving diffusion equation with variable coefficients (5.2) and manufactured solution (5.3). Restart every 25 iterations. Stopping criteria $\eta_{A,b}(x_k) \leq \delta$. $\delta = \epsilon = h^3$. For $h = h_x = h_y \in \{1.56(-2), 7.81(-3), 3.90(-3)\}$, this figure displays the history of solution error, iteration number, $\eta_{A,b}$, solution rank, and maximal Krylov rank.

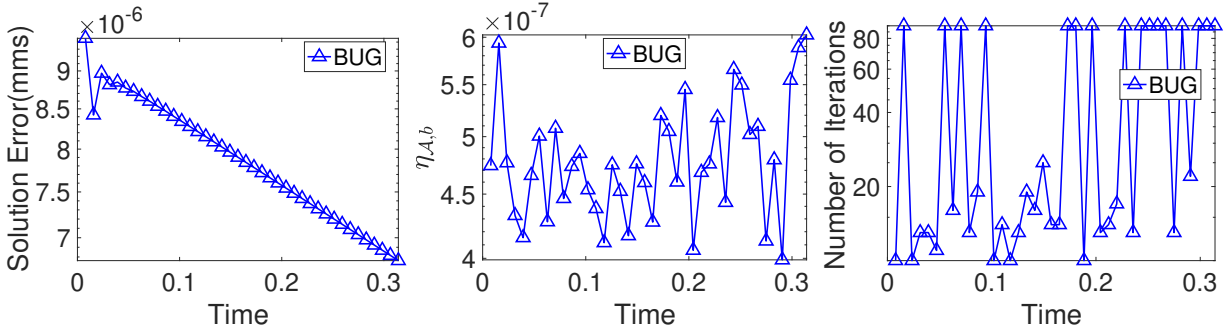


Fig. 4: Example 5.3. Solving diffusion equation with variable coefficients (5.2) and manufactured solution (5.3). Restart every 3 iterations using BUG preconditioner. Stopping criteria $\eta_b \leq \delta$. $\delta = \epsilon = h^3$. For $h = h_x = h_y = 7.81(-3)$, we report the history of solution error, $\eta_{A,b}$, and iteration number.

However, the BUG preconditioner retains its second order convergence rate. The BUG preconditioner has more forgiveness for larger tolerance and this phenomenon is reported in Tables 3 and 4 in later parts of the paper.

In summary, from examples tested in this subsection, we confirm that the optimal parameter shall be taken as the following: stopping criteria $\eta_{A,b}(x_k) \leq \delta$. $\delta = \epsilon$ with ϵ chosen according to local truncation error analysis and with frequent restarting (restart=3). In the remaining part of the paper, we will use this choice for the BUG preconditioner.

5.2. Comparison of BUG, ES, and hybrid preconditioners. In this subsection, we conduct detailed comparison of the performance of the ES, BUG and the hybrid preconditioner. Like the previous subsection, we consider second order in space and time schemes with mesh $\Delta t = O(h)$. The BUG precondi-

h	error (ES)	order (ES)	error (BUG)	order (BUG)
3.12(-2)	1.18(-4)	–	1.11(-4)	–
1.56(-2)	5.16(-5)	1.19	2.84(-5)	1.96
7.81(-3)	3.09(-5)	0.74	7.11(-6)	2.00
3.90(-3)	1.65(-5)	0.91	1.77(-6)	2.00

Table 2: Example 5.4. Solving diffusion equation with variable coefficients (5.2) with manufactured solution (5.3). BUG and ES preconditioner. $\delta = \epsilon = h^2$. For $h = h_x = h_y \in \{3.12(-2), 1.56(-2), 7.81(-3), 3.90(-3)\}$, this table displays the error at the final time and order of convergence.

tioner use the parameter choice indicated in previous subsection. The ES preconditioner use parameters as indicated in the Appendix with the same rounding tolerance as the BUG preconditioner.

The advantage of the ES preconditioner is its computational efficiency based on a simple sum of Kronecker products. However, the accuracy of ES is based on a particular form of operator structure which may not hold in many cases. We note that the BUG preconditioner does have cost associated with solving K-, L- and the Galerkin steps. Ideally, for matrix equations of different size and structures [24], there are various techniques to be used to optimize the computation. In this paper, we did not optimize those solvers, and from our numerical experiments, the result is still satisfactory.

EXAMPLE 5.5. In this example we solve equation (5.1) with the following coefficients

$$(5.4) \quad \begin{aligned} a_1(x) = 1 = b_1(y), & \quad a_2(x) = 0.8 = b_3(y), \\ b_2(y) = 1 = a_3(x), & \quad a_4(x) = 1 = b_4(y), \end{aligned}$$

and manufactured solution

$$(5.5) \quad X(x, y, t) = \exp(-(x - 0.1 \sin(t))^2 / 0.12^2) \exp(-(y + 0.1 \cos(t))^2 / 0.12^2) \exp(-t).$$

Figure 5 displays the simulation results. The three preconditioners perform similarly with regard to the solution error and rank. The BUG and hybrid preconditioner give smaller values for $\eta_{A,b}$. The iteration numbers for the ES preconditioner are constant (=5) independent of the time step. For the BUG preconditioner, the iteration numbers are 1 except the first time step. We notice that this observation is consistent with results reported in the previous subsection. The solution has a rapid transition during the initial layer, and this causes a larger iteration number (=10) initially.

We further test the time stepping with an initial condition where we set $t = 0$ in (5.5) to get

$$(5.6) \quad X(x, y, 0) = \exp(-x^2 / 0.12^2) \exp(-(y + 0.1)^2 / 0.12^2)$$

and no forcing term, i.e. $G(x, y, t) = 0$. We display in Figure 6 the history of $\eta_{A,b}$, the solution rank, the maximal Krylov rank, and the iteration number. In the figure, we also display the solution rank when rounded by the same rounding constant and a full rank standard finite difference scheme in comparison. We can see that the exact solution has a rank that grows at the initial stage and the rank starts to decay. All three preconditioners accurately track this trend in rank. The hybrid preconditioner yields a lower number of iteration and has the smallest maximal Krylov rank.

EXAMPLE 5.6 (High contrast variable coefficient example). We proceed with a challenging example, where we have high contrast variable coefficients give by

$$(5.7) \quad \begin{aligned} a_1(x) = 1, & \quad b_1(y) = 1 + 0.1 \sin(\pi y), \\ a_2(x) = 1, & \quad b_2(y) = 1/\eta(1 + 0.1 \sin(\pi y)), \\ a_3(x) = 1, & \quad b_3(y) = 1/\eta(1 + 0.1 \sin(\pi y)), \\ a_4(x) = 1, & \quad b_4(y) = 1/\eta^2(1 + 0.1 \sin(\pi y)), \end{aligned}$$

with $\eta = 1/10$. We test with the manufactured solution given by

$$(5.8) \quad X(x, y, t) = (1 + \sin(\pi t/2))(1 - x^2)(1 - y^2) \exp(x) \exp(y).$$

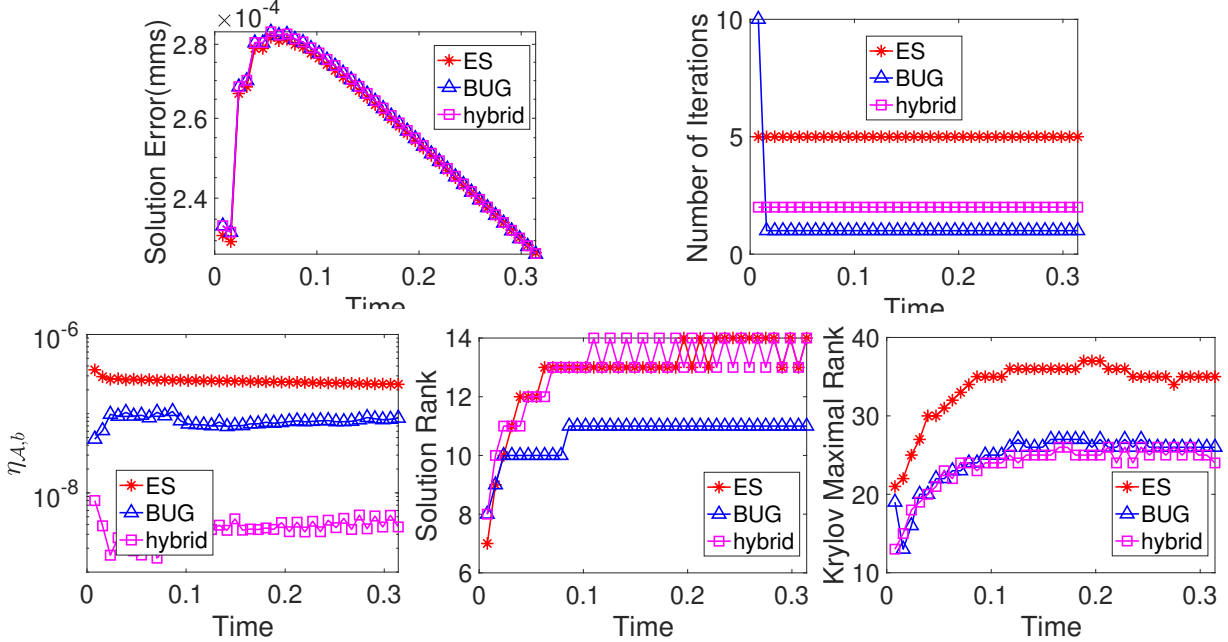


Fig. 5: Example 5.5. Solving diffusion equation with constant coefficients (5.4) and manufactured solution (5.5). Preconditioner: ES, BUG, and hybrid. Rounding tolerance $\epsilon = h^3$. For $h = h_x = h_y = 7.81(-3)$, this figure displays the history of solution error, iteration number, $\eta_{A,b}$, solution rank, and maximal Krylov rank.

	error	order	error	order	error	order	error	order
h	$\epsilon = h^3(\text{ES})$	–	$\epsilon = \eta h^3(\text{ES})$	–	$\epsilon = \eta^2 h^3(\text{ES})$	–	$\epsilon = h^3(\text{BUG})$	–
3.12(-2)	1.42(-2)	–	1.17(-3)	–	9.67(-4)	–	9.13(-4)	–
1.56(-2)	4.77(-3)	1.57	3.10(-4)	1.92	2.35(-4)	2.03	2.40(-4)	1.92
7.81(-3)	4.71(-3)	0.017	9.71(-5)	1.67	6.06(-5)	1.95	6.03(-5)	1.99

Table 3: Example 5.6. Solving diffusion equation with high contrast variable coefficients (5.7) and manufactured solution (5.8). Preconditioner: ES and BUG. For $h = h_x = h_y \in \{3.12(-2), 1.56(-2), 7.81(-3)\}$, this table displays the solution error at the final time for different rounding tolerances and order of convergence.

In Table 3, we test the convergence using rounding tolerance $\epsilon \in \{h^3, \eta h^3, \eta^2 h^3\}$ for the ES preconditioner and $\epsilon = h^3$ for BUG preconditioner. For the ES preconditioner, the second order convergence is achieved when $\epsilon = \eta^2 h^3$ according to the tolerance number chosen according to problem scaling. However, the ES preconditioner fails to converge when $\epsilon = h^3$. The BUG preconditioner, on the other hand, gives the second order convergence rate with $\epsilon = h^3$. This table is similar in spirit to Table 2, which shows BUG preconditioner is more forgiving, and allows a larger choice of ϵ . In Figure 7, we compare ES and BUG preconditioners with $\epsilon = \eta^2 h^3$ and $\epsilon = h^3$ respectively. In those cases, the two preconditioners give similar errors as indicated by Table 3. We can see the BUG preconditioner outperform ES preconditioner in terms of number of iterations and maximal Krylov rank, and solution rank in this case.

5.3. Higher order schemes. In this subsection, we consider higher order schemes. We use a fourth order finite difference spatial discretization with high order single step or multistep method: Crouzeix’s three stage, fourth-order DIRK (diagonally implicit Runge-Kutta) method and fourth order backward differentiation formula (BDF) with mesh $\Delta t = O(h)$. In this case, the local truncation error is on the order of $\Delta t(\Delta t^4 + h^4) = O(h^5)$. For the BDF4 scheme and the inner stage solver for the DIRK4 method, the rounding tolerance ϵ is to make sure that its induced error is on the same order of the local truncation

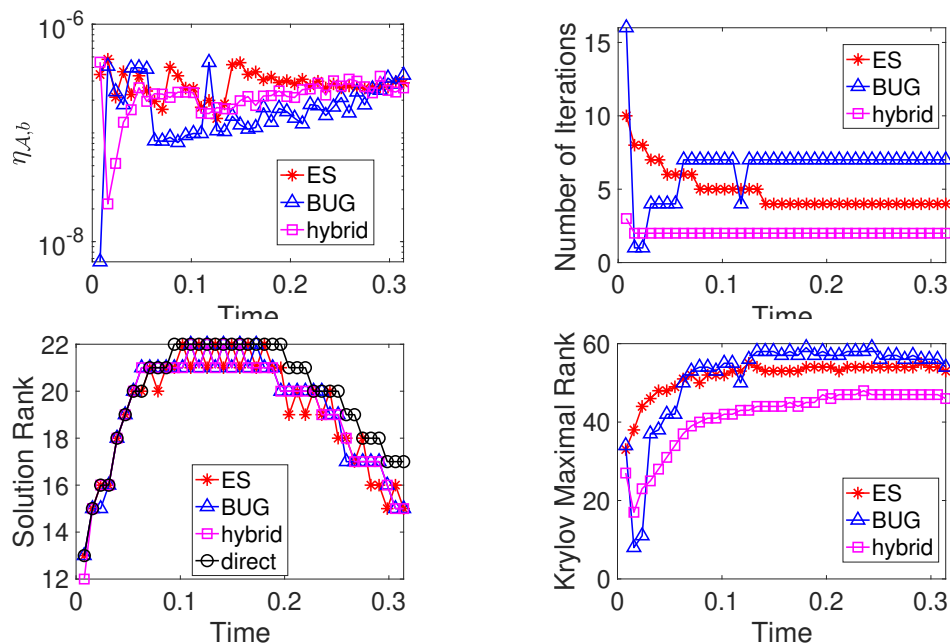


Fig. 6: Example 5.5. Solving diffusion equation with coefficients (5.4) and initial condition (5.6). Preconditioner: ES, mBUG, and hybrid. Rounding tolerance $\epsilon = h^3$. For $h = h_x = h_y = 7.81(-3)$, this figure displays the history of iteration number, $\eta_{A,b}$, solution rank, and maximal Krylov rank.

error, we need $h\epsilon(1 + \Delta t/h^2) = O(h^5)$, which leads to $\epsilon = O(h^5)$. For the truncation tolerance, we take $\epsilon_2 = O(h^4)$ to match the accuracy. To avoid very small rounding tolerance ϵ , we test the algorithms at most to $h = h_x = h_y = 2/2^7$ which already leads to $h^5 = O(10^{-10})$. All other parameters are chosen as recommended in Section 5.1. The final time is $t_{\text{end}} = 0.4\pi$ in this subsection.

We note that to design high order BUG integrators, is highly challenging [20, 5]. Typically one need to add many bases to the K- or L-step to ensure high order accuracy, which will increase the rank and slow down the computation. However, in this framework, this issue is not present any more, which is a major advantage of using the BUG as a preconditioner rather than a direct solver.

EXAMPLE 5.7 (BDF4). We compute with the fourth order BDF scheme and and fourth order spatial discretization for (5.1) with the following variable coefficients

$$(5.9) \quad \begin{aligned} a_1(x) &= 1 + 0.15 \sin(\pi x), & b_1(y) &= 1 + 0.1 \cos(\pi y), \\ a_2(x) &= 0.15 = b_3(y), & b_2(y) &= 1 = a_3(x), \\ a_4(x) &= 1, & b_4(y) &= 1 + 0.1 \cos(\pi y), \end{aligned}$$

and manufactured solution

$$(5.10) \quad X(x, y, t) = \exp(-(x - 0.1 \sin(t))^2/0.12^2) \exp(-(y + 0.1 \cos(t))^2/0.12^2) \exp(-t).$$

Table 4 displays the solution error at the final time for the ES, BUG, and hybrid preconditioners. When rounding tolerance is $\epsilon = h^5$, the fourth-order convergence can be observed for all three preconditioners. However when $\epsilon = h^3$, The ES preconditioner does not converge, while the BUG and hybrid preconditioner still converge with fourth order accuracy. Figure 8 displays the history of solution error, $\eta_{A,b}$, solution rank, maximal Krylov rank, and iteration number for three preconditioners. The Krylov ranks are not small for the ES preconditioner, while the Krylov ranks are smaller for the BUG and hybrid preconditioners.

EXAMPLE 5.8 (Fourth order DIRK). We consider the same problem as above, i.e. coefficients (5.9) and manufactured solution (5.10) with fourth order DIRK scheme and fourth order spatial discretization. We compare the performance of the scheme with two different choice of U, S, V . Those appear in the parameters

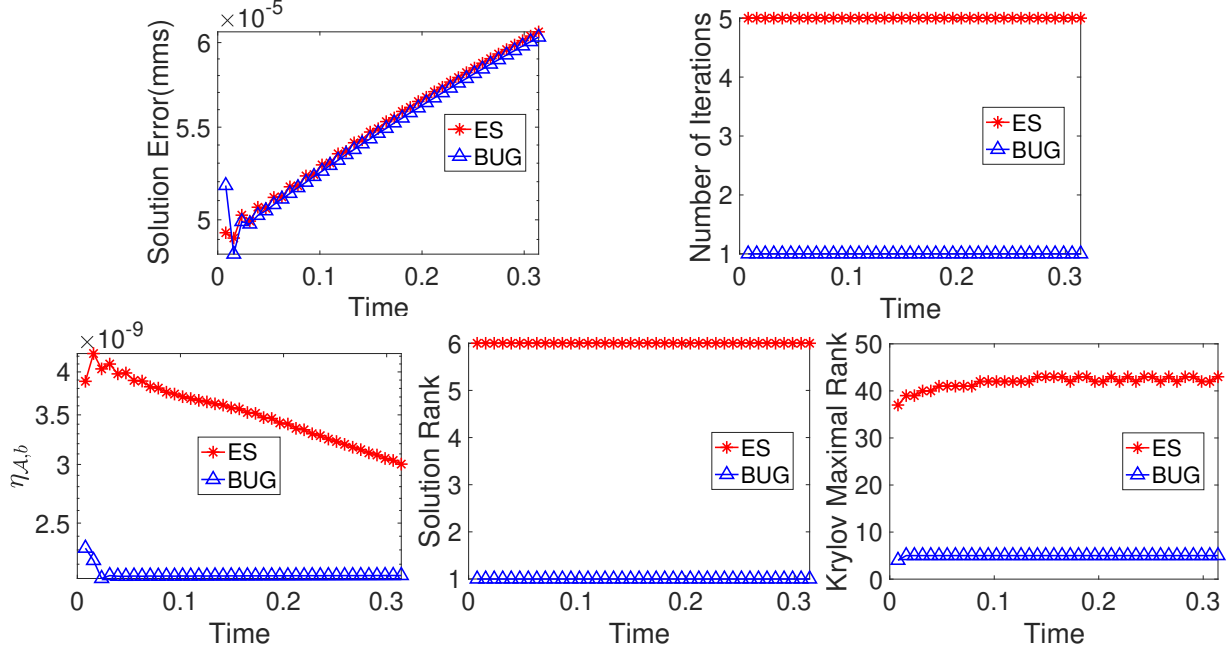


Fig. 7: Example 5.6. Solving diffusion equation with high contrast variable coefficients (5.7) and manufactured solution (5.8). Preconditioner: ES and BUG. Rounding tolerance $\epsilon = \eta^2 h^3$ for ES and $\epsilon = h^3$ for BUG. For $h = h_x = h_y = 7.81(-3)$, this figure displays the history of solution error, iteration number, $\eta_{A,b}$, solution rank, and maximal Krylov rank.

$(\epsilon = h^5)$ h	ES error	ES order	BUG error	BUG order	hybrid error	hybrid order
1.25(-1)	9.49(-3)	–	9.49(-3)	–	9.49(-3)	–
6.25(-2)	4.03(-4)	4.55	4.03(-4)	4.55	4.03(-4)	4.55
3.12(-2)	2.80(-5)	3.84	2.80(-5)	3.84	2.80(-5)	3.84
1.56(-2)	1.81(-6)	3.94	1.81(-6)	3.94	1.81(-6)	3.94
$(\epsilon = h^3)$ h	ES error	ES order	BUG error	BUG order	hybrid error	hybrid order
1.25(-1)	9.33(-3)	–	9.31(-3)	–	9.07(-3)	–
6.25(-2)	4.03(-4)	4.53	4.03(-4)	4.52	4.07(-4)	4.47
3.12(-2)	4.14(-5)	3.28	2.81(-5)	3.84	2.82(-5)	3.84
1.56(-2)	4.97(-5)	-0.26	1.81(-6)	3.95	1.81(-6)	3.96

Table 4: Example 5.7. Solving diffusion equation with variable coefficients (5.9) and manufactured solution (5.10). BDF4 and fourth order finite difference in space. Preconditioner: ES, BUG, and hybrid. For $h = h_x = h_y \in \{1.25(-1), 6.25(-2), 3.12(-2), 1.56(-2)\}$, this table displays the solution error at the final time. Rounding tolerance $\epsilon = h^5$ (top table) and $\epsilon = h^3$ (bottom table).

in the BUG preconditioner, and also as initial guess for the all three preconditioners. Figure 9 and 10 display the history of solution error, $\eta_{A,b}$, solution rank, maximal Krylov rank, and iteration number for three preconditioners. For the iteration number, we sum up the iteration numbers in the three inner stages of DIRK, while the maximal Krylov rank is taken as the maximal for the three stages. In Figure 9, the initial guess for the implicit solvers at DIRK inner stages is taken as the numerical solution X^n , while in Figure 10, it is taken as the inner stage solution at the previous time step, i.e. we use $X^{n-1,(j)}$ which is the j -th inner stage at the previous time step for the current j -th inner stage. We can see a visible difference between the

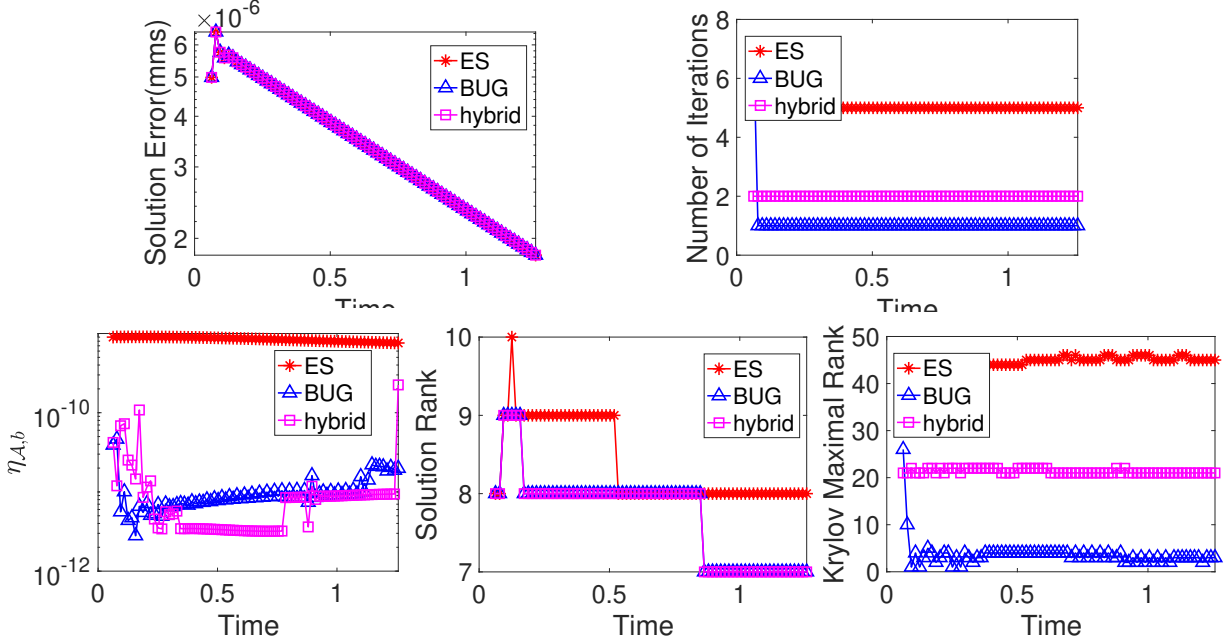


Fig. 8: Example 5.7. Solving diffusion equation with variable coefficient (5.9) and manufactured solution (5.10). BDF4 and fourth order finite difference in space. Preconditioner: ES, BUG, and hybrid. Fourth-order scheme with BDF. Rounding tolerance $\epsilon = h^5$. For $h = h_x = h_y = 1.56(-2)$, this figure displays the history of solution error, iteration number, $\eta_{A,b}$, solution rank, and maximal Krylov rank.

h	ES error	ES order	BUG error	BUG order	hybrid error	hybrid order	full rank error	full rank order
1.25(-1)	8.13(-3)	–	8.19(-3)	–	8.15(-3)	–	8.15(-3)	–
6.25(-2)	4.10(-4)	4.31	4.10(-4)	4.32	4.10(-4)	4.31	4.10(-4)	4.31
3.12(-2)	2.98(-5)	3.78	2.98(-5)	3.78	2.98(-5)	3.78	2.98(-5)	3.78
1.56(-2)	2.38(-6)	3.64	2.38(-6)	3.64	2.38(-6)	3.64	2.38(-6)	3.64

Table 5: Example 5.8. Solving diffusion equation with variable coefficients (5.9) and manufactured solution (5.10). Fourth-order DIRK time stepping and fourth order finite difference in space. Initial guess: $X^{n-1,(j)}$ for updating implicit solver at the j -th inner stage in DIRK. Preconditioner: ES, BUG, and hybrid, in comparison with a full rank solver. This table displays the solution error at the final time and the associated order.

two approaches. With X^n as the initial guess, all three preconditioners give excessively large solution rank, thus large maximal Krylov rank. With initial guess taken as previous inner stage values, the solution rank is at a reasonable value. This example indicates the advantage of using $X^{n-1,(j)}$ as the initial guess for the inner stage of Runge-Kutta methods. For this example, the hybrid conditioner offers the best overall quality in solution rank and maximal Krylov rank. Table 5 displays the solution error at the final time for the ES, BUG, and hybrid preconditioners with initial guess $X^{n-1,(j)}$. All three preconditioners have errors that are similar to a full rank solver.

6. Conclusions and future work. In this work, we propose new preconditioners for the low rank GMRES schemes for implicit time discretization of the matrix differential equations. The preconditioner is based on the BUG method, which is a DLRA of the matrix differential equation on a fixed low rank manifold. The BUG method as a direct solver is subject to the modeling error and does not have convergence guarantee for general problems. On the other hand, when used as a preconditioner, it offers robust performance.

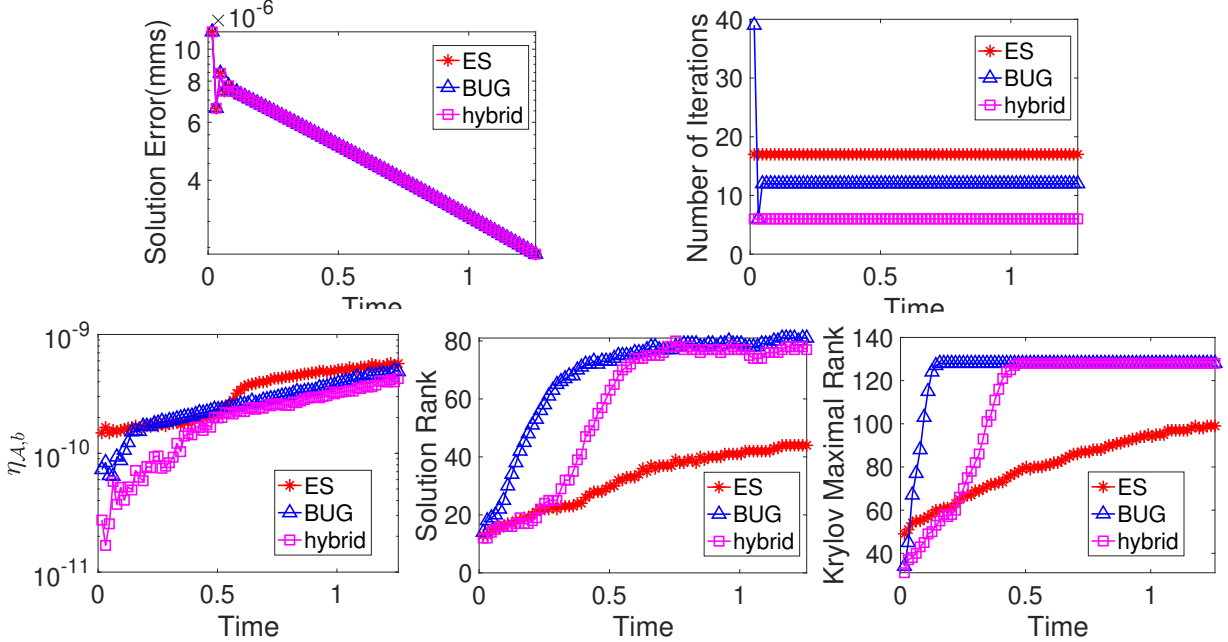


Fig. 9: Example 5.8. Solving diffusion equation with coefficients (5.9) and manufactured solution (5.10). Initial guess: $USV^T = X^n$. Fourth-order DIRK and fourth order finite difference in space. Preconditioner: ES, BUG, and hybrid. Rounding tolerance $\epsilon = h^5$ in implicit solver and h^4 in last step update $X^n \rightarrow X^{n+1}$. For $h = h_x = h_y = 1.56(-2)$, this figure displays the history of solution error, iteration number, $\eta_{A,b}$, solution rank, and maximal Krylov rank. For the iteration number, we sum up the iteration numbers in the three inner stages of DIRK, while the maximal Krylov rank is taken as the maximal for the three stages.

Moreover, the BUG preconditioner framework can easily accommodate arbitrary high order time stepping without the need to augment/enlarge the basis as done in variants of BUG [20, 5].

The BUG preconditioner is a nonlinear preconditioner. We perform a detailed study on its parameters, including tolerance parameter, restart parameter and stopping criteria. We conclude a frequent restart with tolerance selected based on local truncation error of the scheme is effective. This is justified by stability and convergence analysis. We further propose a hybrid version where we alternate between BUG and ES preconditioner. The numerical evidence has suggested that BUG preconditioner and the hybrid version generally require a very low iteration number except for the few initial time steps, and it can control the maximal Krylov rank well. Moreover, compared to the standard ES preconditioner, it is less sensitive to larger rounding tolerance and is blind to the operator being inverted. We show that for the challenging high contrast anisotropic cross diffusion example, the BUG preconditioner is more effective than the ES preconditioner. Future work includes higher dimensional extensions and applications.

Acknowledgment and Disclaimer. This material is based upon work supported by the U.S. Department of Energy, Office of Science, Advanced Scientific Computing Research (ASCR), under Award Number DE-SC0025424, and DOE Mathematical Multifaceted Integrated Capability Centers (MMICC) center grant DE-SC0023164.

This report was prepared as an account of work sponsored by an agency of the United States Government. Neither the United States Government nor any agency thereof, nor any of their employees, makes any warranty, express or implied, or assumes any legal liability or responsibility for the accuracy, completeness, or usefulness of any information, apparatus, product, or process disclosed, or represents that its use would not infringe privately owned rights. Reference herein to any specific commercial product, process, or service by trade name, trademark, manufacturer, or otherwise does not necessarily constitute or imply its endorsement, recommendation, or favoring by the United States Government or any agency thereof. The views and opinions of authors expressed herein do not necessarily state or reflect those of the United States Government or any

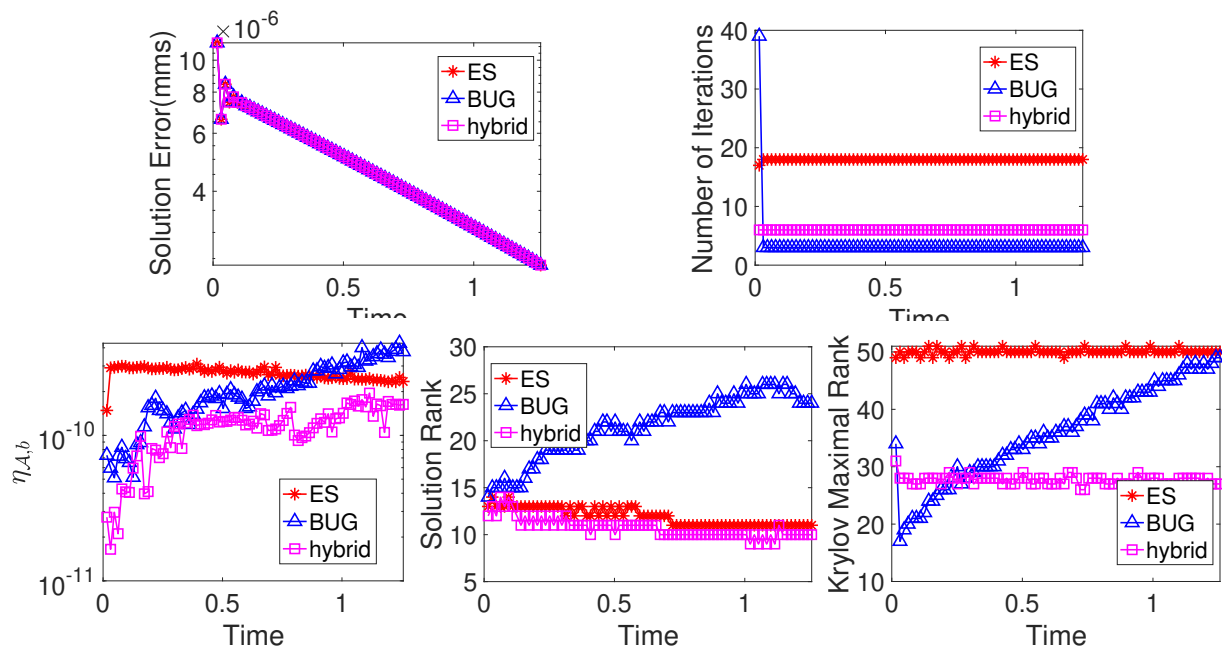


Fig. 10: Example 5.8. Solving diffusion equation with coefficients (5.9) and manufactured solution (5.10). Initial guess: $USV^T = X^{n-1,(j)}$ for updating implicit solver at the j -th inner stage in DIRK. Fourth-order DIRK and fourth order finite difference in space. Preconditioner: ES, BUG, and hybrid. Rounding tolerance $\epsilon = h^5$ in implicit solver and h^4 in last step update $X^{(n)} \rightarrow X^{(n+1)}$. For $h = h_x = h_y = 1.56(-2)$, this figure displays the history of solution error, iteration number, $\eta_{A,b}$, solution rank, and maximal Krylov rank. For the iteration number, we sum up the iteration numbers in the three inner stages of DIRK, while the maximal Krylov rank is taken as the maximal for the three stages.

agency thereof.

REFERENCES

- [1] D. Appelö and Y. Cheng. Robust implicit adaptive low rank time-stepping methods for matrix differential equations. *arXiv:2402.05347*. preprint.
- [2] M. Bachmayr. *Adaptive low-rank wavelet methods and applications to two-electron Schrödinger equations*. PhD thesis, Hochschulbibliothek der Rheinisch-Westfälischen Technischen Hochschule Aachen, 2012.
- [3] M. Bachmayr. Low-rank tensor methods for partial differential equations. *Acta Numerica*, 32:1–121, 2023.
- [4] J. Ballani and L. Grasedyck. A projection method to solve linear systems in tensor format. *Numerical linear algebra with applications*, 20(1):27–43, 2013.
- [5] G. Ceruti, L. Einkemmer, J. Kusch, and C. Lubich. A robust second-order low-rank bug integrator based on the midpoint rule. *BIT Numerical Mathematics*, 64(3):30, Jul 2024.
- [6] G. Ceruti, J. Kusch, and C. Lubich. A rank-adaptive robust integrator for dynamical low-rank approximation. *BIT Numerical Mathematics*, 62(4):1149–1174, 2022.
- [7] G. Ceruti and C. Lubich. An unconventional robust integrator for dynamical low-rank approximation. *BIT Numerical Mathematics*, 62(1):23–44, 2022.
- [8] O. Coulaud, L. Giraud, and M. Iannacito. A robust GMRES algorithm in tensor train format. *arXiv preprint arXiv:2210.14533*, 2022.
- [9] S. V. Dolgov. TT-GMRES: solution to a linear system in the structured tensor format. *Russian Journal of Numerical Analysis and Mathematical Modelling*, 28(2):149–172, 2013.
- [10] L. Grasedyck, D. Kressner, and C. Tobler. A literature survey of low-rank tensor approximation techniques. *GAMM-Mitteilungen*, 36(1):53–78, 2013.
- [11] W. Hackbusch. Solution of linear systems in high spatial dimensions. *Computing and visualization in science*, 17(3):111–118, 2015.
- [12] W. Hackbusch and B. N. Khoromskij. Low-rank Kronecker-product approximation to multi-dimensional nonlocal operators. part i. Separable approximation of multi-variate functions. *Computing*, 76:177–202, 2006.
- [13] W. Hackbusch and B. N. Khoromskij. Low-rank Kronecker-product approximation to multi-dimensional nonlocal operators. part ii. HKT representation of certain operators. *Computing*, 76:203–225, 2006.

- [14] O. Koch and C. Lubich. Dynamical low-rank approximation. *SIAM Journal on Matrix Analysis and Applications*, 29(2):434–454, 2007.
- [15] D. Kressner and P. Sirković. Truncated low-rank methods for solving general linear matrix equations. *Numerical Linear Algebra with Applications*, 22(3):564–583, 2015.
- [16] D. Kressner and C. Tobler. Krylov subspace methods for linear systems with tensor product structure. *SIAM journal on matrix analysis and applications*, 31(4):1688–1714, 2010.
- [17] D. Kressner and C. Tobler. Low-rank tensor Krylov subspace methods for parametrized linear systems. *SIAM Journal on Matrix Analysis and Applications*, 32(4):1288–1316, 2011.
- [18] H. Y. Lam, G. Ceruti, and D. Kressner. Randomized low-rank runge-kutta methods. *arXiv preprint arXiv:2409.06384*, 2024.
- [19] C. Lubich and I. V. Oseledets. A projector-splitting integrator for dynamical low-rank approximation. *BIT Numerical Mathematics*, 54(1):171–188, 2014.
- [20] J. Nakao, J.-M. Qiu, and L. Einkemmer. Reduced augmentation implicit low-rank (rail) integrators for advection-diffusion and fokker-planck models. 11 2023.
- [21] D. Palitta and P. Kürschner. On the convergence of Krylov methods with low-rank truncations. *Numerical Algorithms*, 88(3):1383–1417, 2021.
- [22] A. Rodgers and D. Venturi. Implicit integration of nonlinear evolution equations on tensor manifolds. *Journal of Scientific Computing*, 97(2):33, 2023.
- [23] Y. Saad and M. H. Schultz. GMRES: A generalized minimal residual algorithm for solving nonsymmetric linear systems. *SIAM Journal on scientific and statistical computing*, 7(3):856–869, 1986.
- [24] V. Simoncini. Computational methods for linear matrix equations. *SIAM Review*, 58(3):377–441, 2016.
- [25] V. Simoncini and Y. Hao. Analysis of the truncated conjugate gradient method for linear matrix equations. *SIAM Journal on Matrix Analysis and Applications*, 44(1):359–381, 2023.
- [26] C. Tobler. *Low-rank tensor methods for linear systems and eigenvalue problems*. PhD thesis, ETH Zurich, 2012.

Appendix A. ES preconditioner. We follow [3] to define the ES preconditioner for operators of the form

$$A = \sum_{i=1}^2 \bigotimes_{j=1}^2 B_{i,j}, \quad B_{i,j} = \begin{cases} A_i, & i = j, \\ I, & i \neq j, \end{cases}$$

with self-adjoint and positive definite matrices A_i . The construction of the ES preconditioner that approximates A^{-1} is based on the approximation of

$$\frac{1}{t} = \int_0^\infty e^{-st} ds, \quad t > 0$$

by Sinc quadrature and passing t to A in appropriate sense.

The following Lemma given by [3, Corollary 4.3] states the approximation of t^{-1} by ESs.

LEMMA A.1. *Let $\delta^* = \delta_0 + \eta < 1$ with $\delta_0, \eta \in (0, 1)$, and $T > 1$. With*

$$\alpha = \frac{2\pi}{\ln 3 + |\ln(\cos 1)| + |\ln(\delta_0/2)|},$$

$$m = \lceil \alpha^{-1} \ln |\ln(\delta_0/2)| \rceil, \quad n = \lceil \alpha^{-1} (|\ln(\eta/2)| + \ln T) \rceil,$$

define the ES preconditioner

$$S_{1,\delta_0,\eta,T} = \alpha \sum_{-n}^m e^{k\alpha} \exp(-e^{k\alpha} t).$$

Then

$$|t^{-1} - S_{1,\delta_0,\eta,T}| \leq \delta t^{-1}, \quad \text{for all } t \in [1, T].$$

Passing from t^{-1} to A^{-1} is based on the following Lemma given by [3, Proposition 4.1].

LEMMA A.2. *Let the matrix A be given by*

$$A = \sum_{i=1}^2 \bigotimes_{j=1}^2 B_{i,j}, \quad B_{i,j} = \begin{cases} A_i, & i = j, \\ I, & i \neq j, \end{cases}$$

with self-adjoint and positive definite matrices $A_i \in \mathbb{R}^{N \times N}$ and assume that $\sigma(A) \subset [1, \text{cond}(A)]$. Given a continuous function $\tilde{f} : \mathbb{R}^+ \rightarrow \mathbb{R}^+$, assume that for some $\delta^* \in (0, 1)$ we have $t^{-1} - \tilde{f}(t) \leq \delta t^{-1}$ for all $t \in \sigma(A) \subset [1, \text{cond}(A)]$. Then

$$(1 - \delta^*) \langle A^{-1} v, v \rangle \leq \langle \tilde{f}(A) v, v \rangle \leq (1 + \delta^*) \langle A^{-1} v, v \rangle \text{ for all } v \in \mathbb{R}^N.$$

With the above two lemmas, we are able to estimate the condition number using the ES preconditioner. Let A , $S_{1,\delta_0,\eta,T}$ be given in the above two lemmas with their corresponding assumptions. Then it is expected from [3, Proposition 4.7] that $\text{cond}(AM_{\delta,T})$ can be estimated by $\frac{1+\delta^*}{1-\delta^*}$, where $T \geq \text{cond}(A)$, and

$$\mathcal{M}_{\delta^*,T} = S_{1,\delta^*/2,\delta^*/2,T}(A).$$

In this paper, to define the ES preconditioner for equation (5.1), we consider the diagonal part of the diffusion coefficients, and use their domain averages. Namely, the operator to be used for the ES preconditioner is the approximate inverse corresponding to the scheme for

$$u_t = \overline{a_1 b_1} u_{xx} + \overline{a_4 b_4} u_{yy},$$

where $\overline{\cdot}$ denotes the domain average of the function. This will yield the following type of operator in the time stepping

$$A = I \otimes I - \tau(I \otimes C + D \otimes I),$$

for a given τ (which is related to the time stepping). We simply rewrite the operator as

$$I \otimes (0.5I - \tau C) + (0.5I - \tau D) \otimes I.$$

Let $A_1 = (0.5I - \tau C)$ and $A_2 = (0.5I - \tau D)$, the exponential sum preconditioner reads

$$\mathcal{M}_{\delta^*,T} = \alpha \sum_{-n}^m e^{k\alpha} \exp(-e^{k\alpha} A_2) \otimes \exp(-e^{k\alpha} A_1).$$

The choice of the parameter T depends on the condition number of \mathcal{A} . In our applications, the condition number of \mathcal{A} is on the order of $\mathcal{O}(\tau\eta^{-2}h^{-2})$ and we chose $T = 4\tau\eta^{-2}h^{-2}$, where $\eta = 1/10$ for high contrast and $\eta = 1$ otherwise. We chose empirically $\delta^* = 0.2$ in the numerical examples. For every matrix in SVD form $b = U_b S_b V_b^T$, we round $\mathcal{M}_{\delta^*,T} b$ by the truncation sum algorithm with a given tolerance and a maximal rank. We chose this rounding tolerance the same as the lrGMRES rounding tolerance ϵ .